Supplementary Figure and Table Legends

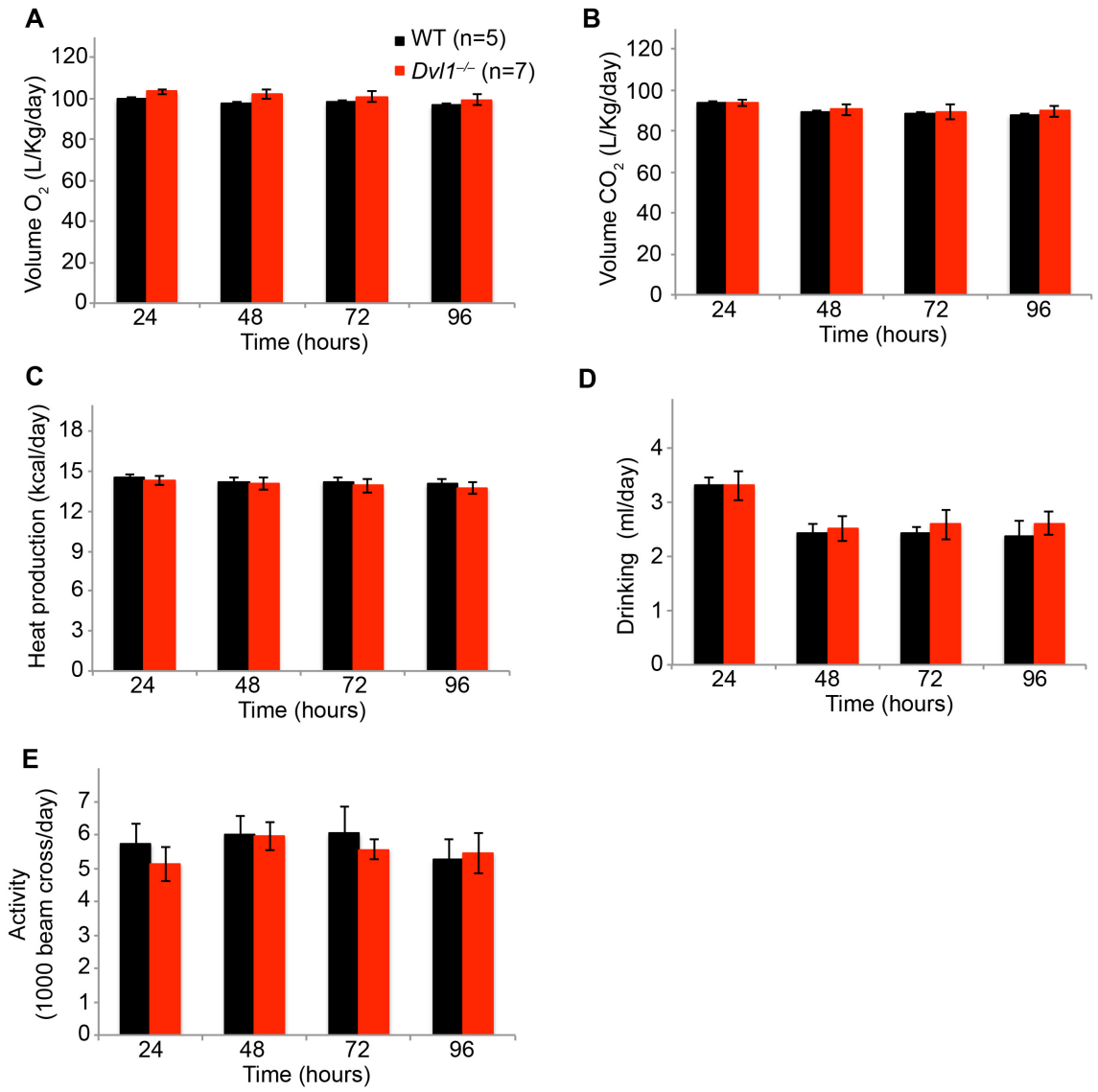

Figure S1: Whole-animal metabolic analysis.
12 week old WT and *Dvl1*$^{-/-}$ were singly housed in CLAMS cages (Comprehensive Laboratory Animals Monitoring System) for 4 days. Measurements of oxygen consumption (A), carbon dioxide output (B), Heat production (C) water consumption (D) and activity (E) were taken every 12 min.

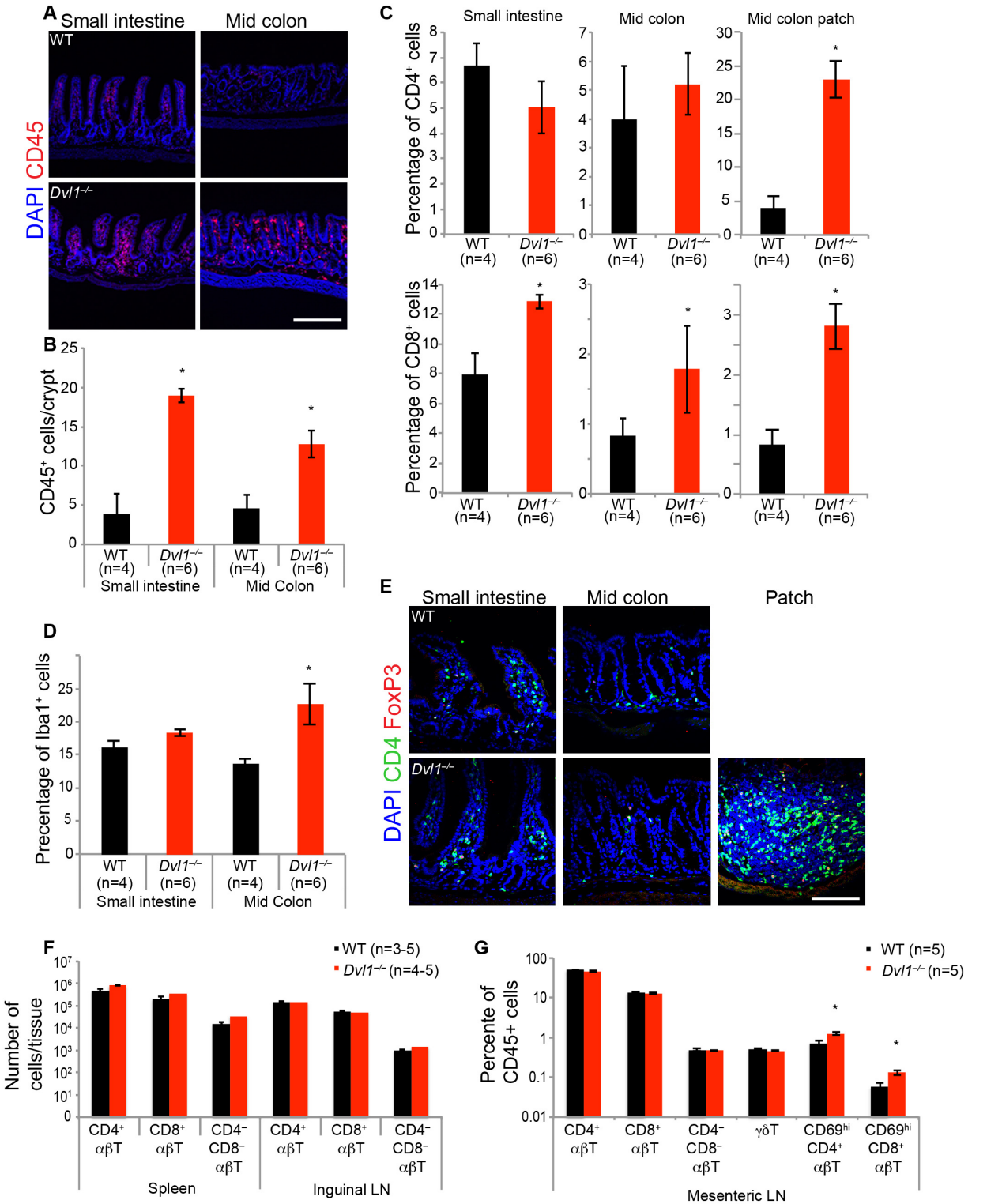

Figure S2: Abnormal inflammatory response in the GI tract of *Dvl1*$^{-/-}$ mice.
12-15 week old WT and *Dvl1*$^{-/-}$ Ileum and proximal colon were processed for flow cytometry and histology (A) Sections from Ileum and proximal colon of WT and *Dvl1*$^{-/-}$ mice were stained with DAPI and CD45, and representative images are shown (Scale bar: 100μm). (B) Quantification of the number of DAPI^{+}CD45^{+} labeled cells per crypt are

presented as mean±SEM (*p<0.02 for comparing the results of the *Dvl1*$^{-/-}$ with those of the WT mice). (C) Sections from GI tract of WT and *Dvl1*$^{-/-}$ mice were stained with DAPI, CD4 and CD8 and quantification of the percentage of DAPI^{+}CD4^{+} or DAPI^{+}CD8^{+} labeled cells in the lamina propria of the Ileum, mid colon and patch region are presented as mean±SEM (*p<0.04 for comparing the results of the *Dvl1*$^{-/-}$ with those of the WT mice). (D) Sections from Ileum and mid colon of WT and *Dvl1*$^{-/-}$ mice were stained with DAPI and Iba-1 (macrophages), and quantification of the percentage of DAPI^{+}Iba-1^{+} labeled cells in the lamina propria are presented as mean±SEM (*p<0.04 for comparing the results of the *Dvl1*$^{-/-}$ with those of the WT mice). (E) Sections from Ileum and proximal colon of WT and *Dvl1*$^{-/-}$ mice were stained with DAPI, CD4 and FoxP3 and representative images are shown (Scale bar: 100μm). (F-G) Spleen, inguinal lymph node and mesenteric lymph node of 15 week old WT and *Dvl1*$^{-/-}$ mice were processed for flow cytometry. Lymphoid cell markers were used to determine (F) the number of a specific lymphoid cell population per cm tissue and (G) the percentage of CD45^{+} cells. Results are presented as mean±SEM. (*p<0.02 for comparing the results of the *Dvl1*$^{-/-}$ with those of the WT mice)

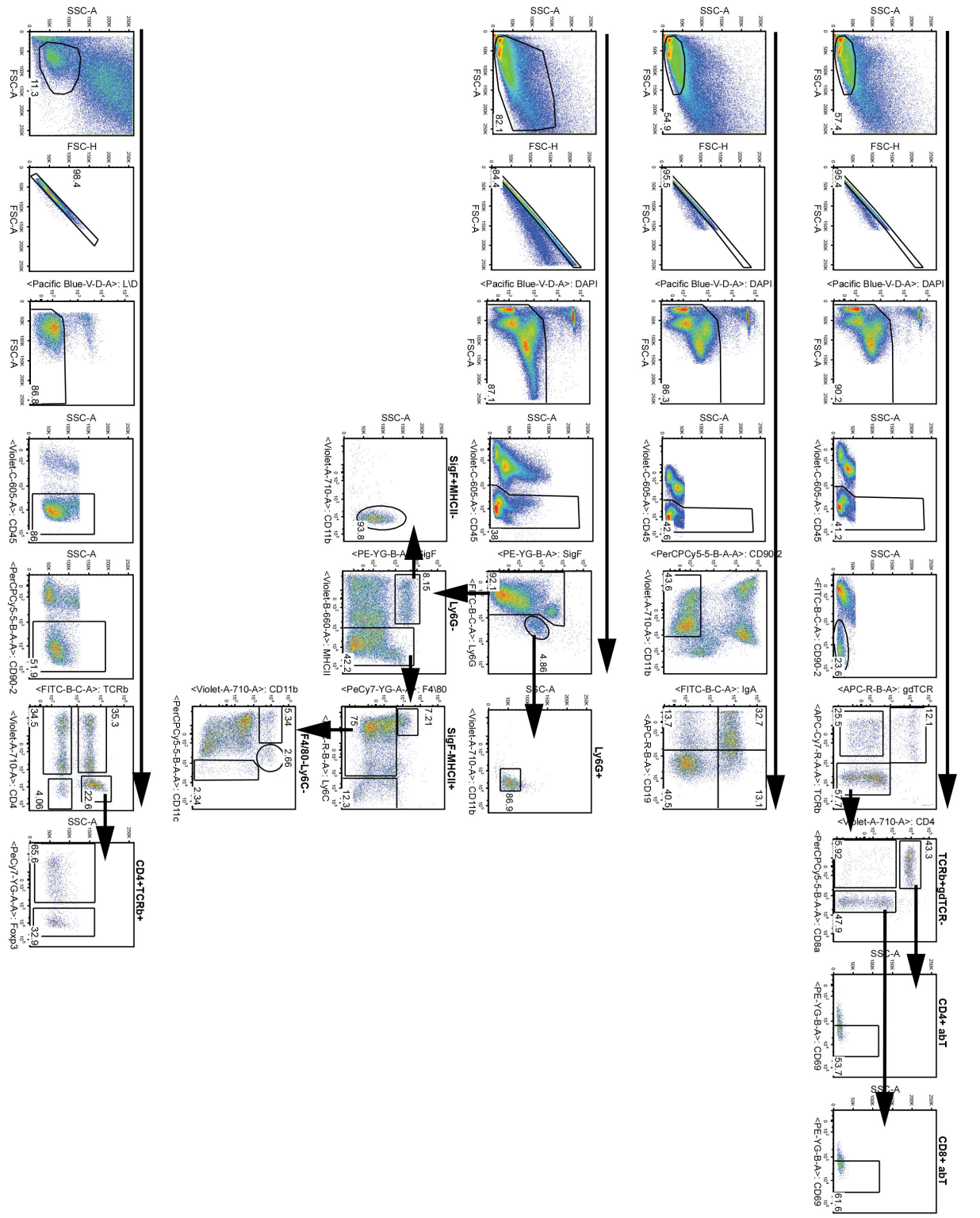

Figure S3: Gating scheme for lymphoid and myeloid cell populations.
The GI tracts of 15 week old WT and *Dvl1*$^{-/-}$ mice were prepared for flow cytometry; large intestine and small intestine were dissected individually. The gating scheme was used to measure the lymphoid and myeloid cell populations.

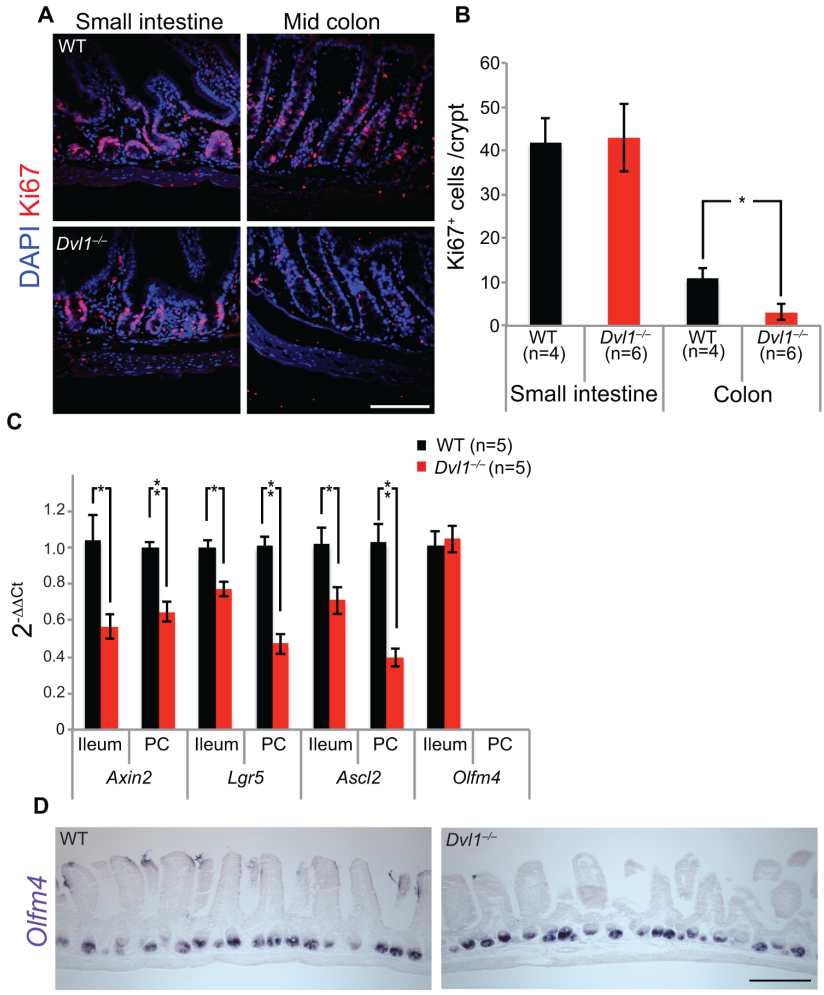

Figure S4: Epithelial cell composition in the GI tract of *Dvl1*$^{-/-}$ mice.
The GI tract of WT and *Dvl1*$^{-/-}$ mice were processed for histology, RT-PCR and in-situ hybridization. (A) Sections from the GI tract of 12 weeks old mice were immunostained with DAPI and Ki67 and representative images are shown. (Scale bar: 100μm). (B) Quantification of the number of DAPI^{+}Ki67^{+} labeled cells per crypt are presented as mean±SEM (*p<0.03 for comparing the results of the *Dvl1*$^{-/-}$ with those of the WT mice). (C) RNA from ileum and proximal colon (PC) of 12 week old WT and *Dvl1*$^{-/-}$ mice was extracted and RT-PCR was performed. The levels of *Axin2*, *Lgr5*, *Ascl2*, and *Olfm4* were normalized to *Gapdh* and are presented as mean±SEM (n=5; *p<0.05 and **p<0.005 for comparing the results of the *Dvl1*$^{-/-}$ with those of the WT mice). (D)The GI tract of 8 week-old WT and *Dvl1*$^{-/-}$ mice were processed for *in situ* hybridization. Sections from the GI tract were probed for *Olfm4* and representative images are shown (Scale bar: 200μm).

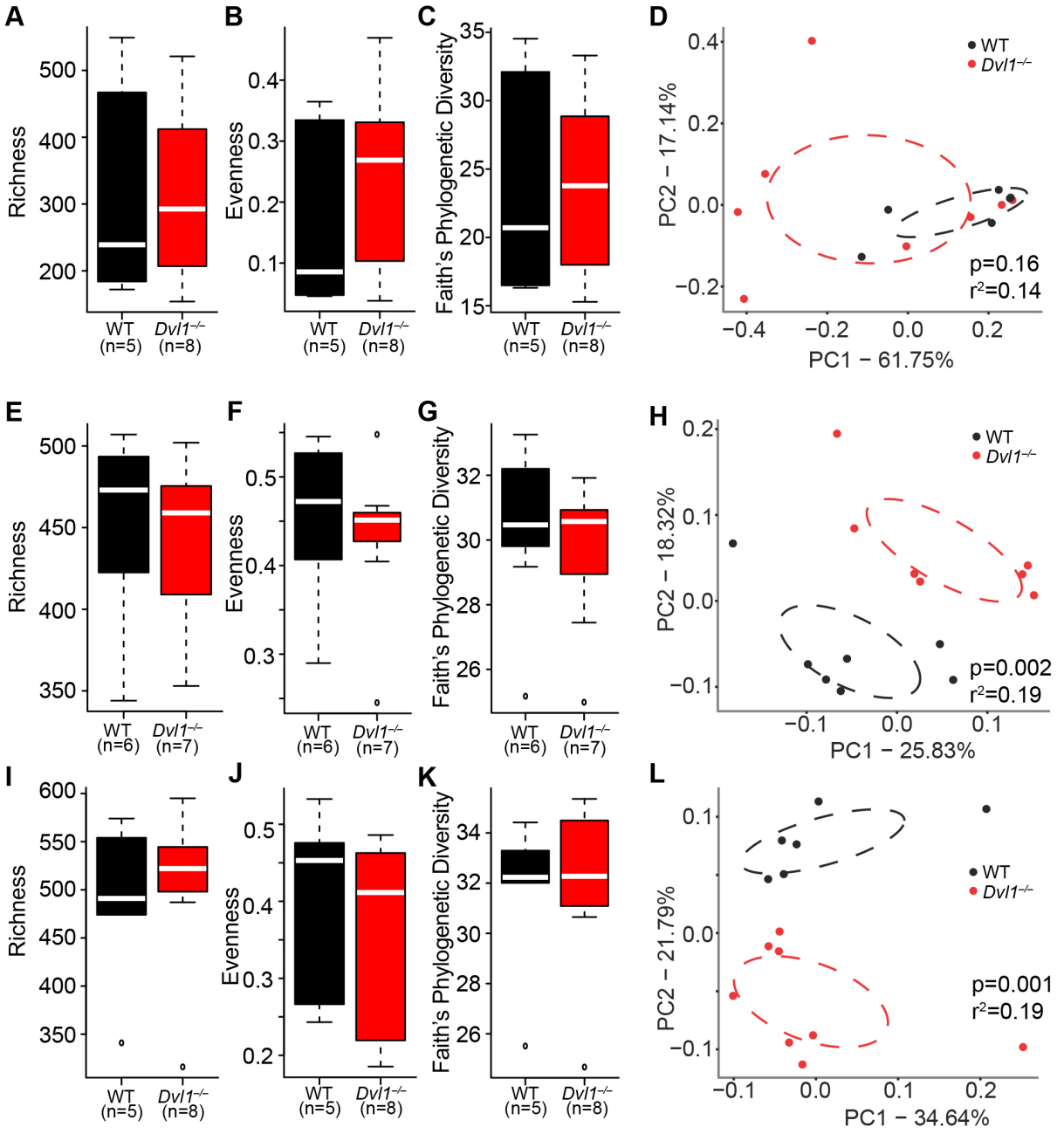

Figure S5: Microbiome composition in *Dvl1*$^{-/-}$ mice.
(A-C) Ileum of 12 week old WT and *Dvl1*$^{-/-}$ mice 16S rRNA gene profiling of alpha diversity indices (phylotype richness, Pileau's evenness and Faith's phylogenetic diversity) was analyzed and compared to WT mice. Results are presented as box-plots. (D) 16S rRNA gene profiling of beta diversity from Ileum of individual 12 week old WT and *Dvl1*$^{-/-}$ mice using weighted UniFrac distance matrix is presented. (E-G) Mid-colon of 6 week old WT and *Dvl1*$^{-/-}$ mice 16S rRNA gene profiling of alpha diversity indices (phylotype richness, Pileau's evenness and Faith's phylogenetic diversity) was analyzed compared to WT mice. Results are presented as box-plots. (H) 16S rRNA gene profiling of beta diversity from Mid-colon of individual 6 week old WT and *Dvl1*$^{-/-}$ mice using unweighted UniFrac distance matrix is presented. Permanova statistical analysis

revealed significant difference (p=0.002) in microbiota composition of *Dvl1*$^{-/-}$ and WT mice. (I-K) Mid-colon of 12 week old WT and *Dvl1*$^{-/-}$ mice 16S rRNA gene profiling of alpha diversity indices (phylotype richness, Pileau's evenness and Faith's phylogenetic diversity) was analyzed compared to WT mice. Results are presented as box-plots. (L) 16S rRNA gene profiling of beta diversity from Mid-colon of individual 12 week old WT and *Dvl1*$^{-/-}$ mice using unweighted UniFrac distance matrix is presented. Permanova statistical analysis revealed significant difference (p=0.001) in microbiota composition of *Dvl1*$^{-/-}$ and WT mice.

Table S1: Significantly enriched OTUs identified in WT and *Dvl1*$^{-/-}$ mice.
Ileum and proximal colon of WT and *Dvl1*$^{-/-}$ mice were processed for 16S rRNA gene profiling and the relative abundance of the significantly different OTUs are shown.

Table S2: Significantly enriched OTUs identified in co-housed mice.
Ileum and proximal colon of standard and co-housed WT and *Dvl1*$^{-/-}$ mice were processed for 16S rRNA gene profiling and the relative abundance of the significantly different OTUs are shown.

Table S3: Significantly enriched OTUs identified in supplemented and unsupplemented *Dvl1*$^{-/-}$ mice.
Ileum and proximal colon of PBS and L. Jonhsonaii fed WT and *Dvl1*$^{-/-}$ mice were processed for 16S rRNA gene profiling and the relative abundance of the significantly different OTUs are shown.